European Journal of Radiology 85 (2016) 1512–1518

Contents lists available at ScienceDirect

European Journal of Radiology

journal homepage: www.elsevier.com/locate/ejrad

# MR-based assessment of body fat distribution and characteristics☆

Thomas Baum[a,*], Christian Cordes[a], Michael Dieckmeyer[a], Stefan Ruschke[a], Daniela Franz[a], Hans Hauner[b,c], Jan S. Kirschke[d], Dimitrios C. Karampinos[a]

[a] Department of Diagnostic and Interventional Radiology, Klinikum rechts der Isar, Technische Universität München, Munich, Germany
[b] Else Kröner Fresenius Center for Nutritional Medicine, Klinikum rechts der Isar, Technische Universität München, Munich, Germany
[c] ZIEL Research Center for Nutrition and Food Sciences, Technische Universität München, Germany
[d] Section of Diagnostic and Interventional Neuroradiology, Klinikum rechts der Isar, Technische Universität München, Munich, Germany

ARTICLE INFO

*Article history:*
Received 29 December 2015
Received in revised form 3 February 2016
Accepted 9 February 2016

*Keywords:*
Body fat distribution
Body fat characteristics
Magnetic resonance imaging
Fat imaging

ABSTRACT

The assessment of body fat distribution and characteristics using magnetic resonance (MR) methods has recently gained significant attention as it further extends our pathophysiological understanding of diseases including obesity, metabolic syndrome, or type 2 diabetes mellitus, and allows more detailed insights into treatment response and effects of lifestyle interventions. Therefore, the purpose of this study was to review the current literature on MR-based assessment of body fat distribution and characteristics. PubMed search was performed to identify relevant studies on the assessment of body fat distribution and characteristics using MR methods. T1-, T2-weighted MR Imaging (MRI), Magnetic Resonance Spectroscopy (MRS), and chemical shift-encoding based water-fat MRI have been successfully used for the assessment of body fat distribution and characteristics. The relationship of insulin resistance and serum lipids with abdominal adipose tissue (i.e. subcutaneous and visceral adipose tissue), liver, muscle, and bone marrow fat content have been extensively investigated and may help to understand the underlying pathophysiological mechanisms and the multifaceted obese phenotype. MR methods have also been used to monitor changes of body fat distribution and characteristics after interventions (e.g. diet or physical activity) and revealed distinct, adipose tissue-specific properties. Lastly, chemical shift-encoding based water-fat MRI can detect brown adipose tissue which is currently the focus of intense research as a potential treatment target for obesity. In conclusion, MR methods reliably allow the assessment of body fat distribution and characteristics. Irrespective of the promising findings based on these MR methods the clinical usefulness remains to be established.



## 1. Introduction

The metabolic syndrome is a constellation of interrelated risk factors of metabolic origin that directly increases the risk of cardiovascular disease and type 2 diabetes mellitus [1]. Among others visceral adiposity, dyslipidemia (elevated triglycerides and low high-density lipoprotein (HDL)), elevated fasting glucose and hypertension are metabolic risk factors which constitute the metabolic syndrome [2]. Metabolic syndrome, type 2 diabetes mellitus, and overweight/obesity are associated with increased mortality and due to their high prevalence are classified as public health problems with severe socio-economic consequences. Particularly, overweight and obesity are considered as an epidemic, and projections have suggested that 86.3% of adults in the United States will be overweight or obese by 2030 [3].

Body fat distribution has been identified as an important diagnostic and prognostic marker for the onset, progression, and mortality risk of these diseases [4–7]. The assessment of body fat distribution traditionally relied on anthropometric measurements, e.g. body mass index (BMI), waist circumference, or waist-to-hip ratio, and/or broadly available clinical tools, e.g. bioelectric impedance machines. However, the obese phenotype is multifaceted and anthropometric measurements are unable to assess regional body fat distribution and characteristics [8,9]. Similarly, bioelectric impedance machines cannot assess regional compartments of body fat and their characteristics [10,11].

Assessment of body fat composition can be performed with imaging techniques including Dual energy X-ray Absorptiometry (DXA), Computed Tomography (CT), Magnetic Resonance (MR) methods (MR Imaging (MRI) and MR Spectroscopy (MRS)) [12,13]. While DXA can only differentiate bone, fat, and lean soft tissue, CT allows the determination of adipose tissue volumes, i.e.

☆ MeSH Unique ID: D050218; D008279; D009765; D024821; D003920

* Corresponding author at: Department of Diagnostic and Interventional Radiology, Klinikum rechts der Isar, Technische Universität München, Ismaninger Str. 22, 81675 Munich, Germany.
*E-mail address:* thbaum@gmx.de (T. Baum).

http://dx.doi.org/10.1016/j.ejrad.2016.02.013
0720-048X/

subcutaneous and visceral adipose tissue (SAT and VAT), and the amount of fat deposition in the liver and skeletal muscle [12–14]. MR offers the possibility to perform these CT measurements without ionizing radiation [12;13]. Furthermore, even more sophisticated parameters including extra- and intramyocellular lipid and bone marrow fat characteristics can be assessed by using MRS, thus allowing a dedicated phenotyping with regard to regional body fat distribution and their characteristics [15].

Therefore, the purpose of this study was to review the current literature on MR-based assessment of regional body fat distribution and characteristics.

## 2. MR-based assessment of body fat distribution and characteristics

### 2.1. Literature search

Keyword search was performed using PubMed (http://www.ncbi.nlm.nih.gov/pubmed) up to November 2015 to identify relevant studies for this review. No starting date was entered for the electronic search to obtain the entire literature available in PubMed. Search terms used included "body fat distribution"; "body fat characteristics"; "ectopic fat"; "obesity"; "metabolic syndrome"; "diabetes"; "adipose tissue"; "fat imaging"; "magnetic resonance imaging"; and "$^{1}$H-based magnetic resonance spectroscopy". The search was restricted to studies in humans. The reference lists of relevant articles were also screened.

### 2.2. Adipose tissue classification

To date, there is no generally accepted classification of adipose tissues in humans. However, Shen et al. proposed an imaging-based classification of the topography of adipose tissue [16]: Total adipose tissue (TAT) is the sum of adipose tissue, usually excluding bone marrow and adipose tissue in the head, hands, and feet. Subcutaneous adipose tissue (SAT) is defined as the layer between the dermis and the aponeuroses and fasciae of the muscles including the mammary adipose tissue. Internal adipose tissue (IAT) results from the subtraction of SAT from TAT and consists of visceral adipose tissue (VAT) and non-visceral IAT. VAT refers to the adipose tissue within the chest, abdomen, and pelvis, non-visceral IAT mainly to intra- and perimuscular adipose tissue. The paraosseal and intermuscular adipose tissue constitutes the perimuscular adipose tissue. Importantly, Shen et al. observed inconsistencies in the use of specific definitions, especially for the compartment termed "visceral" adipose tissue. Furthermore, MR allows the quantification and characterization of organ, ectopic, and bone marrow fat as well as the differentiation of white and brown fat.

### 2.3. MR methods

Relaxometry- and chemical shift-based MR methods have been reported to accurately and reliably assess body fat distribution and characteristics [17,18].

T1-weighted imaging is differentiating proton signals from water and fat due to their different T1 relaxation times. Adipose tissue appears bright on T1-weighted images and has been used for the quantification of SAT, VAT, bone marrow fat, and intermuscular adipose tissue (IMAT). Advantages of T1-weighted imaging are the broad availability throughout MR scanners, high spatial resolution, and strong water-fat tissue contrast, disadvantages the sensitivity to B1 inhomogeneities and partial volume effects. The computation of the adipose tissue volumes require (semi-) automatic segmentation techniques based on signal intensity histograms and thresholds [19]. Depending on the segmentation algorithm, SAT and VAT reproducibility measurements were not found to differ significantly, e.g. Kullberg et al. reported mean and standard deviation of $2.0 \pm 14\%$ for VAT and $0.84 \pm 2.7\%$ for SAT measurements, respectively [20]. Importantly, T1-weighted imaging has been broadly used in the assessment of muscular fat infiltration in neuromuscular disorders [21,22].

T2-weighted imaging is differentiating proton signals from water and fat due to their different T2 relaxation times with fat appearing hyperintense. It has been mainly used for fat quantification in the lower extremity muscles and is not suitable for SAT and VAT determination. Advantages and drawbacks are similar to those of T1-weighted imaging.

Single-voxel $^{1}$H-based MRS has been considered as non-invasive gold standard for ectopic fat quantification using PRESS (point resolved spectroscopy) or STEAM (stimulated echo acquisition mode) sequences. Water and fat signals are identified by their chemical shift locations along the frequency spectrum. MRS has been widely used to measure proton density fat fraction (PDFF) in the liver, skeletal muscle, and bone marrow and has been also recently used to measure fatty acid composition, e.g. the degree of unsaturation or presence of omega-3 fatty acids. MRS-based hepatic PDFF measurements were reproducible across field strengths (1.5 T versus 3 T) with mean intra-examination standard deviations of 0.49% and mean inter-examination standard deviations of 0.46% [23,24]. Short- and long-term reproducibility measurements of intra- and extramyocellular lipids in the skeletal muscle using MRS ranged from 19% to 33% [25]. Reproducibility of MRS-based bone marrow fat fraction was reported as coefficient of variation of 1.7% at the lumbar spine [26]. The accurate assessment of bone marrow unsaturation level is challenging due to overlapping water-fat peaks. Therefore, it may be more beneficial to use diffusion-weighted STEAM instead of long-TE PRESS for measuring fat unsaturation in regions with low PDFF [27].

Chemical shift encoding-based water-fat MRI allows fat quantification with high spatial resolution which is advantageous compared to single-voxel MRS as the distribution of fat content can be spatially heterogeneous, particularly in the bone marrow [28]. To improve the reliable extraction of imaging-based PDFF, it has been shown to use a low flip angle to reduce bias from T1 relaxation, acquire multiple echoes to perform correction for T2* decay, and apply a prior known fat spectrum to model the spectral complexity of fat [29]. Modeling of T2* decay effects is of particular importance when measuring PDFF in the liver in the presence of iron and in bone marrow in the presence of trabecular bone [30]. Recent studies have shown a good agreement between water-fat imaging and single-voxel MRS-based bone marrow PDFF when confounding factors are taken into account, e.g. T2* effects [30,31]. Reproducibility of water-fat imaging-based PDFF amounted 1.7% averaged over C3-L5 [32]. Similarly, reproducibility of water-fat imaging-based liver PDFF has been reported to be excellent (standard deviation of $\leq$0.66%) [33]. Furthermore, chemical shift encoding-based water-fat MRI offers the possibility of a separate assessment of inter- and intramuscular fat, thus overcoming an important limitation of T1-weighted imaging. The intra-observer reproducibility of water-fat imaging-based intramuscular fat fraction generated by manual segmentation at the calf amounted 2.7% [34]. Lastly, SAT and VAT volume can be determined by using water-fat imaging (Fig. 1). Wald et al. presented an automated segmentation algorithm for a 2-point Dixon sequence and reported coefficients of variation from repeated measurements of $3.50 \pm 2.93\%$ for VAT and $0.35 \pm 0.26\%$ for SAT, respectively [35].

### 2.4. SAT and VAT

Ludescher et al. performed whole-body T1-weighted imaging in 68 volunteers and determined several adipose tissue volumes

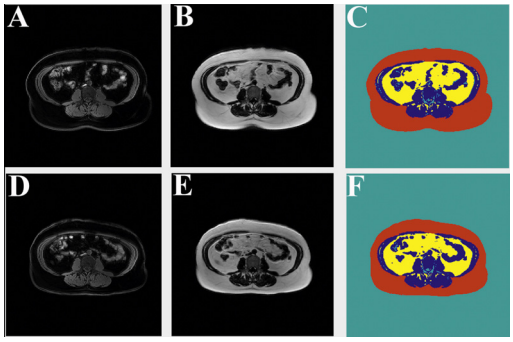


**Fig. 1.** Representative axial 2-point Dixon water-fat imaging at baseline (A–C) and after a 4-week dietary intervention (D–F) in an obese woman. A and D: water images, B and E: fat images; C and F: automatic segmentation of SAT (red), VAT (yellow), air/bone (cyan) and non-adipose tissue (blue).
Dixon images based on a 3D spoiled gradient echo sequence with imaging parameters: TR = 4.0 s, TE1/TE2 = 1.32/2.6 ms, flip angle = 10°, bandwidth = 1004 Hz/pixel, acquisition matrix size = 332 × 220, FOV = 500 × 446 mm$^2$, acquisition voxel = 1.5 × 2.0 × 5.0 mm$^3$, 44 slices, parallel imaging using SENSE with a reduction factor R = 2.5.

including SAT and VAT [36]. Furthermore, they assessed body fat content with different modalities including skinfold caliper, body impedance, and simple anthropometric data (i.e. waist-to-hip ratio and BMI). The authors reported significant correlations between different body measures and body fat devices with MRI-derived SAT. However, correlations with VAT volume were much weaker. Therefore, the authors concluded that MRI-based assessment of VAT cannot be substituted by simpler methods. This finding is important as VAT is particularly known to increase the risk of metabolic disturbances and cardiovascular disease.

The size of VAT was reported to be the strongest determinant of insulin sensitivity [37]. Kirchhoff et al. performed T1-weighted MRI to measure SAT and VAT in 220 subjects. Insulin sensitivity was derived from an oral glucose tolerance test and correlated significantly with SAT (r = −0.35) and VAT (r = −0.43). Importantly, besides high liver fat, VAT volume was the strongest predictor of low insulin sensitivity in multivariate regression models.

Kanaley et al. investigated regional differences in abdominal fat loss in 33 obese postmenopausal women with type 2 diabetes [38]. The SAT/VAT ratio was determined in T1-weighted images using a single slice (1 cm slice thickness) at L2-L3, five slices (5 × 1 cm slice thickness) centered at L4-L5, and full abdominal coverage (25 cm). The intervention consisted of a 14-week weight loss program by diet alone, exercise alone, or diet and exercise combined. The authors reported a greater relative VAT loss in the L2-L3 region and concluded that if only the L2-L3 region is analyzed the overall VAT loss may be overestimated. Therefore, the investigated region for SAT/VAT measurements has to be carefully considered when using the relatively time consuming T1-weighted imaging. Alternatively, water-fat imaging of the entire abdomen with a single breath hold can be performed to overcome this limitation, e.g. a scan time of 10.6 s was reported by Cordes et al. using a 2-point Dixon sequence [39]. However, most studies investigating the effect of interventions on SAT and VAT were performed by using T1-weighted imaging as water-fat imaging is an emerging method and T1-weighted imaging has been broadly available for a long time.

MRI-based assessment of SAT and VAT has been performed in multiple studies to determine the effects of different interventions [40]. Gallagher et al. included 54 females and 38 males with type 2 diabetes mellitus enrolled in the Look AHEAD (Action for Health in Diabetes) trial in their study [41]. They investigated the effects of a 1-year intensive lifestyle intervention or diabetes support and education on total body fat including SAT and VAT assessed by MRI. In the intensive lifestyle intervention group, SAT and VAT volumes were significantly reduced after 1 year, whereas SAT and VAT volumes remained unchanged in the diabetes support and education group. Interestingly, females had a greater reduction in SAT than males and males showed a greater reduction in VAT than females after intensive lifestyle intervention. Bacchi et al. assigned 40 subjects with type 2 diabetes mellitus to aerobic training or resistance training [42]. They reported that both, resistance training and aerobic training, similarly reduced MRI-based SAT and VAT volumes as well as improved insulin sensitivity.

SAT and VAT were also determined in newborns and young infants, where whole-body MRI is challenging without sedation [43–46]. These studies used T1-weighted or PD-weighted water-saturated fast-spin echo imaging, as these sequences provide a consistent noise level; attempts to use faster sequences failed as infants frequently woke up due to the inconsistent noise level [43]. In young infants reproducibility for TAT and SAT ranged between 2.5% and 3.4% [43,45]. Due to motion and breathing artifacts, reproducibility was much smaller for internal adipose tissue (17.6% to 18.6%) [43,45].

Lastly, single-voxel MRS allows free fatty acid profiling of abdominal adipose tissue. Schrover et al. determined polyunsaturated fatty acids, total unsaturated fatty acids, triglycerides, and their ratios in 12 obese and 13 lean subjects [47]. Polyunsaturated fatty acids/total unsaturated fatty acids and polyunsaturated fatty acids/triglycerides ratios were significantly greater in omental adipose tissue in obese subjects compared to lean subjects ($35 \times 10^{-3}$ versus $0.16 \times 10^{-3}$ and $2.05 \times 10^{-3}$ versus $0.01 \times 10^{-3}$, respectively). The authors suggested that high levels of polyunsaturated fatty acids may reflect a more proinflammatory status of adipose tissue, thus allowing the early identification of adipose tissue dysfunction by using single-voxel MRS. Machann et al. investigated VAT volume by using T1-weighted imaging and its fraction of unsaturated fatty acids by using single-voxel MRS in 12 subjects [48]. They observed an inverse correlation of fraction of unsaturated fatty acids in VAT and total VAT volume (r = −0.92).

### 2.5. Liver fat

Dong et al. recruited 14 subjects with impaired glucose tolerance and 42 glucose-tolerant healthy subjects [49]. They performed water-fat imaging to determine liver fat fraction and reported significant correlations between BMI, waist-to-hip ratio, low-density lipoprotein (LDL), fasting plasma insulin, homeostasis model assessment (HOMA) insulin resistance and liver fat fraction (up to r = 0.89). Kirchhoff et al. performed MRS of the liver to obtain the liver fat fraction and an oral glucose tolerance test to determine insulin sensitivity in 220 subjects [37]. Liver fat fraction and insulin sensitivity showed a significant correlation with r = −0.53. Besides VAT volume, a high liver fat content was the strongest determinant of insulin sensitivity in multivariate regression models. Similarly, Linder et al. reported that the MRS-based liver fat fraction is an independent predictor of insulin resistance in overweight/obese adolescents [50].

MRS-based liver fat fraction has been used as gold standard to predict non-alcoholic fatty liver disease and liver fat by using metabolic and genetic factors [51]. Furthermore, MRS-based liver fat fraction plays a major role in risk stratification for the development of type 2 diabetes mellitus. This is due to several studies investigating factors which were able to predict an increase in insulin sensitivity following intervention: Machann et al. recruited 243 subjects (99 men and 144 women) at increased risk for type 2 diabetes mellitus [52]. All subjects underwent a 9-month lifestyle intervention program that included optimized nutrition and controlled physical activity. T1-weighted imaging was performed to assess SAT and VAT volumes and MRS to determine liver fat fraction at baseline and 9-month follow-up. The most pro-

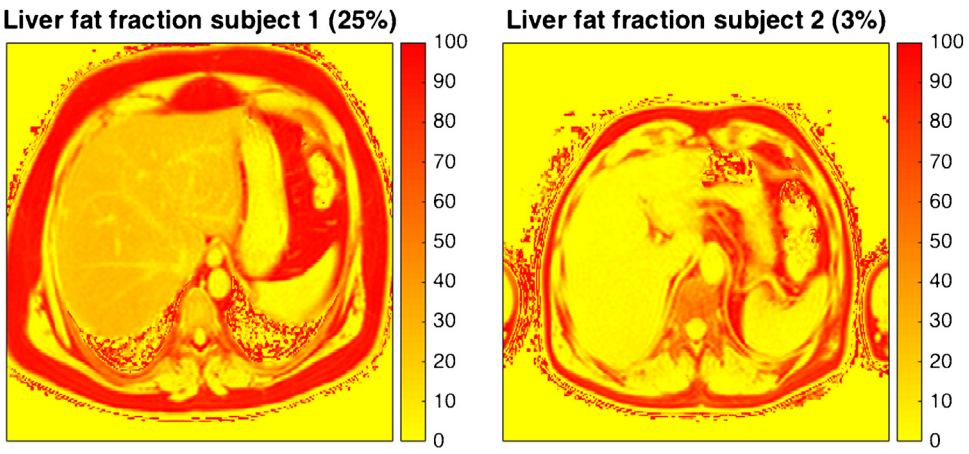


**Fig. 2.** Water-fat imaging-based liver fat fraction maps in a pre-diabetic (1) and healthy (2) subject. Note the elevated liver fat fraction in the pre-diabetic subject (25%) compared to the healthy subject (3%).
A six-echo gradient echo sequence (mDixon quant) was used to measure liver fat fraction with imaging parameters: TR = 7.8 ms, TE1/ΔTE = 1.3/1.1 ms, flip angle = 3°, bandwidth = 1523 Hz/pixel, acquisition matrix size = 152 × 133, FOV = 300 × 403 mm$^2$, acquisition voxel = 2.0 × 3.0 × 6.0 mm$^3$, 25 slices, parallel imaging using SENSE with a reduction factor R = 2.2 × 1.2 (in L/R and F/H respectively).

nounced changes in adipose tissue were reported for VAT (in men: decrease from 4.9 L to 4.1 L, i.e. −15.1%; in women: decrease from 2.3 L to 1.9 L, i.e. −15.8%) and liver fat fraction (in men: decrease from 8.6% to 5.4%, i.e. −36.8%; in women: decrease from 5.1% to 4.3%, i.e. −16.5%). Interestingly, low baseline liver fat levels were significantly predictive of successful intervention in terms of improvement of insulin sensitivity. Kantartzis et al. investigated metabolically benign and insulin-resistant obese subjects by using SAT and VAT measurements (based on T1-weighted imaging) and liver fat (based on MRS) [53]. They included 262 non-diabetic individuals who underwent a 9-month lifestyle intervention program. Obese subjects were stratified into quartiles based on their insulin sensitivity estimated from an oral glucose tolerance test. Subjects in the upper quartile (n = 26) were defined as metabolically benign obese and subjects in the lower three quartiles (n = 77) as insulin-resistant obese. While VAT significantly decreased in metabolically benign and insulin-resistant obese subjects, a reduction in liver fat and improvement of insulin sensitivity were only observed in insulin-resistant obese subjects after intervention. Therefore, identification of the obese phenotype is critical, and MRS-based liver fat may play an important role (Fig. 2).

### 2.6. Skeletal muscle fat

Boettcher et al. investigated the association of intermuscular adipose tissue (IMAT) with other fat depots including VAT and insulin sensitivity [54]. They recruited 249 subjects at increased risk for type 2 diabetes mellitus. Insulin sensitivity was expressed as glucose infusion rate necessary to maintain normoglycemia during the last 60 min of the hyperinsulinemic euglycemic clamp. T1-weighted imaging of the right calf was performed to determine IMAT by subtracting the area of subcutaneous from total adipose tissue. Furthermore, subjects underwent single-voxel MRS in the tibialis anterior muscle to measure intramyocellular lipid (IMCL) content. IMAT showed significant correlations with other fat depots, particularly VAT (r = 0.52 in females; r = 0.42 in males) and insulin sensitivity (r = −0.43 in females; r = −0.40 in males), while IMCL was associated with insulin sensitivity in females only (r = −0.44). Thus, IMAT may be involved in the pathogenesis of insulin resistance.

Sinha et al. compared the intra- and extramyocellular lipid (IMCL and EMCL) content assessed by MRS in the soleus muscle in 14 obese adolescents and 8 non-obese controls [55]. They reported that IMCL and EMCL content were significantly greater in the obese subjects compared to the lean controls. Furthermore, IMCL and EMCL showed inverse correlations with insulin sensitivity (r = −0.59; r = −0.53, respectively). As these findings were found in adolescents, they are most likely not a consequence of aging but are actually expressed early in the natural course of obesity.

Machann et al. performed MRS-based IMCL measurements in the tibialis anterior and soleus muscle in 243 subjects who were at increased risk for type 2 diabetes mellitus [52]. All subjects underwent a 9-month lifestyle intervention program that included optimized nutrition and increased physical activity. They observed a reduction of IMCL content in the tibialis anterior muscle (by 12.3% in men and by 6.9% in women) and soleus muscle (by 13% in men and by 12.3% in women). However, baseline IMCL level in neither muscle group significantly correlated with subsequent change in insulin sensitivity.

Karampinos et al. assessed the spatial distribution of skeletal muscle adipose tissue in the calf by using chemical shift-encoding based water-fat MRI in subjects with type 2 diabetes mellitus and healthy age-matched controls [56]. Water-fat imaging is advantageous compared to T1-weighted imaging as IMAT can be divided into two separate compartments, i.e. fat within the muscular regions (intraMF) and fat between the muscular regions (interMF). The authors reported no statistically significant difference in the IMAT volume between the two groups. However, the intraMF volume normalized by the IMAT volume was significantly greater in the diabetic subjects compared to the controls. Thus, water-fat imaging reveals important information about the spatial distribution of skeletal adipose tissue which is not captured by T1-weighted imaging.

### 2.7. Bone marrow fat

The association of bone marrow adiposity and bone health has become of increasing interest recently (Figs. 3 and 4).

Griffith et al. recruited 18 women with normal bone density, 30 with osteopenia, and 55 with osteoporosis [57]. MRS-based vertebral marrow fat content in L3 was significantly increased in the osteoporotic group (67.8 ± 8.5%) compared to the normal bone density group (59.2 ± 10.0%). Similar results were observed in men [58].

Bredella et al. recruited 47 premenopausal women (BMI range: 18–41 kg/m$^2$), performed MRS of L4 to measure bone marrow fat

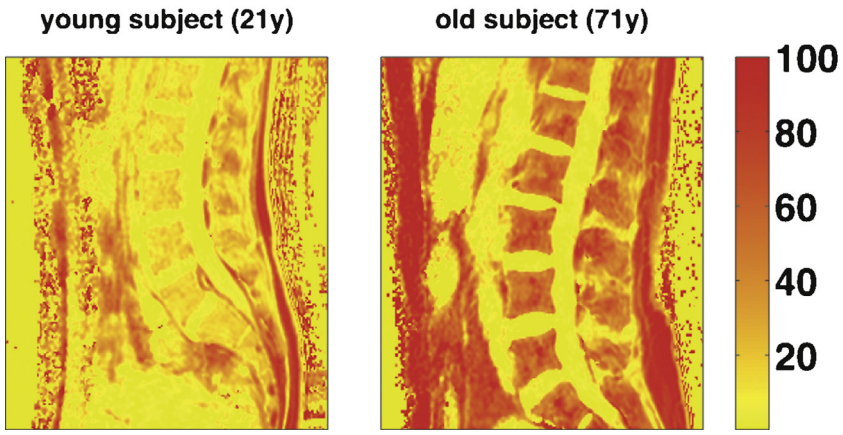


**Fig. 3.** Water-fat imaging-based lumbar spine bone marrow fat fraction maps in a young (left) and an old (right) subject showing an increased bone marrow fat fraction in the old subject.
The 3D spoiled gradient echo sequence acquired eight echoes in two interleaves (4 echoes per TR) using flyback (monopolar) read-out gradients with imaging parameters: $TR/TE_{min}/\Delta TE = 15/1.47/1.05$ ms, flip angle = 3°, bandwidth = 1551 Hz/pixel, acquisition matrix size = 124 × 122, FOV = 220 × 220 mm², slice thickness = 4 mm, slice locations = 20, no parallel imaging.

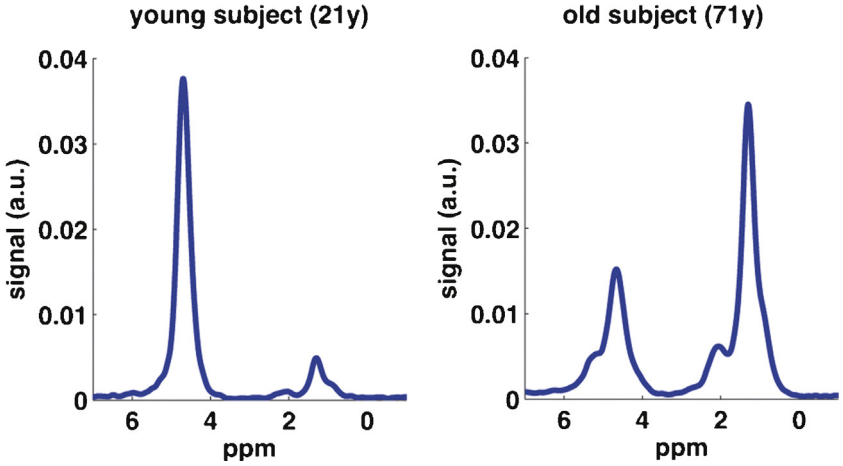


**Fig. 4.** MR spectra of L5 in a young (left) and an old (right) subject. Note the superposition of the mythylene (—$(CH_2)_n$—) peak at 1.30 ppm and the β-carboxyl (—CO—$CH_2$—$CH_2$—) peak at 1.59 ppm, the superposition of the α-olefinic (—$CH_2$—CH=CH—$CH_2$—) peak at 2.00 ppm and the α-carboxyl (—CO—$CH_2$—$CH_2$—) peak at 2.25 ppm, the water peak at 4.7 ppm, and the oelefinic (—CH=CH—) peak at 5.3 ppm. Bone marrow fat fraction was greater in the old compared to the young subject.
A stimulated echo acquisition mode (STEAM) single-voxel MRS sequence was used with imaging parameters: voxel size = 15 × 15 × 5 mm³, TR = 6 s, TM = 16 ms, TE = 11/15/20/25 ms, eight averages per TE, 4096 sampling points, 5 kHz acquisition bandwidth, no water suppression and no regional saturation bands.

content, assessed VAT and bone mineral density by using CT, and determined growth hormone (GH) and insulin-like growth factor 1 (IGF-1) level [59]. Vertebral bone marrow fat content significantly correlated with VAT ($r = 0.34$), and inversely with bone mineral density ($r = -0.39$) and IGF-1 ($r = -0.39$). The authors concluded that the detrimental effect of VAT on bone health may be mediated in part through IGF-1 as an important regulator of the fat and bone lineage.

Another study by Bredella et al. investigated the association of L4 bone marrow fat content with IMCL content in the soleus muscle, intrahepatic lipid content, and serum lipid levels in 106 healthy young men and women [60]. Adipose tissue measurements were performed by using single-voxel MRS. Bone marrow fat content was significantly correlated with intrahepatic lipid content ($r = 0.21$), IMCL ($r = 0.27$), serum HDL level ($r = -0.21$), and serum triglyceride level ($r = 0.33$), independent of BMI, age, insulin resistance, and exercise status. Thus, ectopic fat and serum lipid levels are related with the bone marrow fat and may negatively influence bone health.

Baum et al. performed MRS-based vertebral bone marrow fat quantifications of L1-3 in 13 postmenopausal women with type 2 diabetes mellitus and 13 age- and BMI-matched healthy controls [61]. They determined not only bone marrow fat content, but also bone marrow fat unsaturation level. Mean vertebral bone marrow fat content was similar in the diabetic subjects and healthy controls (69.3 ± 7.5% versus 67.5 ± 6.1%; $p > 0.05$). However, mean bone marrow fat unsaturation level was significantly reduced in the diabetic subjects compared to healthy controls (6.7 ± 1.0% versus 7.9 ± 1.6%; $p < 0.05$). Furthermore, HbA1c correlated significantly with mean vertebral bone marrow fat content in the diabetic subjects ($r = 0.83$). The authors concluded that vertebral bone marrow fat composition may be a biomarker for the quality of glycemic control and potentially for late diabetic complications.

Cordes et al. investigated the effect of a 4-week dietary intervention providing a formula diet with 800 kcal/d plus additional vegetables on MRS-based vertebral bone marrow fat content in 20 obese women (BMI: 34.92 ± 3.8 kg/m²) [39]. They reported no statistically significant changes in vertebral bone marrow fat content after dietary intervention. However, absolute changes in vertebral bone marrow fat content were positively associated with SAT volume ($r = 0.49$) and negatively associated with non-adipose tissue volume ($r = -0.49$) before dietary intervention. Thus, bone marrow fat is related to other fat depots, but seems to exhibit also distinct,

tissue-specific properties and remains an interesting field for future research.

### 2.8. Brown fat and "browning" of white adipose tissue

Brown adipose tissue (BAT) is responsible for thermogenesis and characterized as an extensively vascularized fat tissue with great amounts of iron-containing mitochondria [62]. It is metabolically active mainly throughout early childhood, but can also be found in adults. It shows a characteristic anatomical distribution along large internal arteries and is also localized in the supraclavicular region. Interestingly, recent studies suggested that within white adipose tissue (WAT) depots "browning" can be induced under specific metabolic conditions and, most strongly, upon cold exposure [63]. These inducible brown fat cells, also named beige or brite fat, are currently the focus of intense research as a possible novel treatment option for obesity. It should be noted that beige fat cells are not from the same developmental lineage as classical brown adipocytes. Positron emission tomography (PET) has traditionally been used for the detection of brown fat. However, its application is limited due to the radiation exposure. Franz et al. retrospectively evaluated 66 PET/MR imaging scans of 33 pediatric patients [64]. Imaging included a 2-point Dixon water-fat separation method. BAT and WAT could be differentiated by their signal-fat fraction values due to their different water content. The authors were able to demonstrate that signal-fat fraction values of BAT were independent from its metabolic activity. Thus, signal-fat fraction may be a more reliable parameter for BAT than the commonly used PET signal, but MR imaging of BAT has to be further elaborated in the future.

## 3. Conclusions

Different MR methods are currently available for the assessment of body fat distribution and characteristics. They have been used in multiple research studies to gain insights into the pathophysiology of metabolic diseases including obesity, metabolic syndrome, or type 2 diabetes mellitus. The perspectives are promising, but this field of research is still in an experimental stage and the usefulness of the MR methods for physicians in clinical medicine is still rather limited.

## Conflict of interest

The authors state no conflict of interest.

## Role of the funding sources

Grants of Philips Healthcare and the European Research Council (ERC) partly provide salary support for the authors' research groups.

## Acknowledgements

This work was supported by grants of Philips Healthcare (to D.C.K.), ERC-StG-2014 637164 "iBack" (to J.S.K.) and ERC-StG-2015 677661 "ProFatMRI" (to D.C.K.).

## References

[1] K.G. Alberti, R.H. Eckel, S.M. Grundy, P.Z. Zimmet, J.I. Cleeman, K.A. Donato, J.C. Fruchart, W.P. James, C.M. Loria, S.C. Smith Jr., Harmonizing the metabolic syndrome: a joint interim statement of the International Diabetes Federation Task Force on Epidemiology and Prevention; National Heart, Lung, and Blood Institute; American Heart Association; World Heart Federation; International Atherosclerosis Society; and International Association for the Study of Obesity, Circulation 120 (16) (2009) 1640–1645.

[2] J. Kaur, A comprehensive review on metabolic syndrome, Cardiol. Res. Pract. 2014 (2014) 943162.

[3] Y. Wang, M.A. Beydoun, L. Liang, B. Caballero, S.K. Kumanyika, Will all Americans become overweight or obese? Estimating the progression and cost of the US obesity epidemic, Obesity (Silver Spring) 16 (10) (2008) 2323–2330.

[4] G. Chen, C. Liu, F. Chen, J. Yao, Q. Jiang, N. Chen, H. Huang, J. Liang, L. Li, L. Lin, Body fat distribution and their associations with cardiovascular risk, insulin resistance and beta-cell function: are there differences between men and women? Int. J. Clin. Pract. 65 (5) (2011) 592–601.

[5] J.B. Moller, M. Pedersen, H. Tanaka, M. Ohsugi, R.V. Overgaard, J. Lynge, K. Almind, N.M. Vasconcelos, P. Poulsen, C. Keller, K. Ueki, S.H. Ingwersen, B.K. Pedersen, T. Kadowaki, Body composition is the main determinant for the difference in type 2 diabetes pathophysiology between Japanese and Caucasians, Diabetes Care 37 (3) (2014) 796–804.

[6] J.P. Reis, C.A. Macera, M.R. Araneta, S.P. Lindsay, S.J. Marshall, D.L. Wingard, Comparison of overall obesity and body fat distribution in predicting risk of mortality, Obesity (Silver Spring) 17 (6) (2009) 1232–1239.

[7] Y.C. Hwang, T. Hayashi, W.Y. Fujimoto, S.E. Kahn, D.L. Leonetti, M.J. McNeely, E.J. Boyko, Visceral abdominal fat accumulation predicts the conversion of metabolically healthy obese subjects to an unhealthy phenotype, Int. J. Obes. (Lond.) 39 (9) (2015) 1365–1370.

[8] A. Scafoglieri, J.P. Clarys, E. Cattrysse, I. Bautmans, Use of anthropometry for the prediction of regional body tissue distribution in adults: benefits and limitations in clinical practice, Aging Dis. 5 (6) (2014) 373–393.

[9] M.J. Muller, M. Lagerpusch, J. Enderle, B. Schautz, M. Heller, A. Bosy-Westphal, Beyond the body mass index: tracking body composition in the pathogenesis of obesity and the metabolic syndrome, Obes. Rev. 13 (Suppl. 2) (2012) 6–13.

[10] U. Mulasi, A.J. Kuchnia, A.J. Cole, C.P. Earthman, Bioimpedance at the bedside: current applications, limitations, and opportunities, Nutr. Clin. Pract. 30 (2) (2015) 180–193.

[11] A. Bosy-Westphal, W. Later, B. Hitze, T. Sato, E. Kossel, C.C. Gluer, M. Heller, M.J. Muller, Accuracy of bioelectrical impedance consumer devices for measurement of body composition in comparison to whole body magnetic resonance imaging and dual X-ray absorptiometry, Obes. Facts 1 (6) (2008) 319–324.

[12] L.A. Seabolt, E.B. Welch, H.J. Silver, Imaging methods for analyzing body composition in human obesity and cardiometabolic disease, Ann. N. Y. Acad. Sci. 1353 (1) (2015) 41–59.

[13] H. Wang, Y.E. Chen, D.T. Eitzman, Imaging body fat: techniques and cardiometabolic implications, Arterioscler. Thromb. Vasc. Biol. 34 (10) (2014) 2217–2223.

[14] S. Petak, C.G. Barbu, E.W. Yu, R. Fielding, K. Mulligan, B. Sabowitz, C.H. Wu, J.A. Shepherd, The Official Positions of the International Society for Clinical Densitometry: body composition analysis reporting, J. Clin. Densitom. 16 (4) (2013) 508–519.

[15] E.L. Thomas, J.R. Parkinson, G.S. Frost, A.P. Goldstone, C.J. Dore, J.P. McCarthy, A.L. Collins, J.A. Fitzpatrick, G. Durighel, S.D. Taylor-Robinson, J.D. Bell, The missing risk: MRI and MRS phenotyping of abdominal adiposity and ectopic fat, Obesity (Silver Spring) 20 (1) (2012) 76–87.

[16] W. Shen, Z. Wang, M. Punyanita, J. Lei, A. Sinav, J.G. Kral, C. Imielinska, R. Ross, Heymsfield SB: Adipose tissue quantification by imaging methods: a proposed classification, Obes. Res. 11 (1) (2003) 5–16.

[17] H.H. Hu, H.E. Kan, Quantitative proton MR techniques for measuring fat, NMR Biomed. 26 (12) (2013) 1609–1629.

[18] J. Machann, A. Horstmann, M. Born, S. Hesse, F.W. Hirsch, Diagnostic imaging in obesity, Best Pract. Res. Clin. Endocrinol. Metab. 27 (2) (2013) 261–277.

[19] H.H. Hu, J. Chen, W. Shen, Segmentation and quantification of adipose tissue by magnetic resonance imaging, MAGMA (2015), http://dx.doi.org/10.1007/s10334-015-0498-z (Epub ahead of print).

[20] J. Kullberg, H. Ahlstrom, L. Johansson, H. Frimmel, Automated and reproducible segmentation of visceral and subcutaneous adipose tissue from abdominal MRI, Int. J. Obes. (Lond.) 31 (12) (2007) 1806–1817.

[21] E. Mercuri, A. Pichiecchio, J. Allsop, S. Messina, M. Pane, F. Muntoni, Muscle MRI in inherited neuromuscular disorders: past, present, and future, J. Magn. Reson. Imaging 25 (2) (2007) 433–440.

[22] B.T. Addeman, S. Kutty, T.G. Perkins, A.S. Soliman, C.N. Wiens, C.M. McCurdy, M.D. Beaton, R.A. Hegele, C.A. McKenzie, Validation of volumetric and single-slice MRI adipose analysis using a novel fully automated segmentation method, J. Magn. Reson. Imaging 41 (1) (2015) 233–241.

[23] N.S. Artz, W.M. Haufe, C.A. Hooker, G. Hamilton, T. Wolfson, G.M. Campos, A.C. Gamst, J.B. Schwimmer, C.B. Sirlin, S.B. Reeder, Reproducibility of MR-based liver fat quantification across field strength: same-day comparison between 1.5T and 3T in obese subjects, J. Magn. Reson. Imaging 42 (3) (2015) 811–817.

[24] A. Tyagi, O. Yeganeh, Y. Levin, J.C. Hooker, G.C. Hamilton, T. Wolfson, A. Gamst, A.K. Zand, E. Heba, R. Loomba, J. Schwimmer, M.S. Middleton, C.B. Sirlin, Intra- and inter-examination repeatability of magnetic resonance spectroscopy, magnitude-based MRI, and complex-based MRI for estimation of hepatic proton density fat fraction in overweight and obese children and adults, Abdom. Imaging 40 (8) (2015) 3070–3077.

[25] M.C. Stephenson, E. Leverton, E.Y. Khoo, S.M. Poucher, L. Johansson, J.A. Lockton, J.W. Eriksson, P. Mansell, P.G. Morris, I.A. MacDonald, Variability in fasting lipid and glycogen contents in hepatic and skeletal muscle tissue in subjects with and without type 2 diabetes: a 1H and 13C MRS study, NMR Biomed. 26 (11) (2013) 1518–1526.

[26] X. Li, D. Kuo, A.L. Schafer, A. Porzig, T.M. Link, D. Black, A.V. Schwartz, Quantification of vertebral bone marrow fat content using 3 Tesla MR

spectroscopy: reproducibility, vertebral variation, and applications in osteoporosis, J. Magn. Reson. Imaging 33 (4) (2011) 974–979.
[27] S. Ruschke, H. Kienberger, T. Baum, H. Kooijman, M. Settles, A. Haase, M. Rychlik, E.J. Rummeny, D.C. Karampinos, Diffusion-weighted stimulated echo acquisition mode (DW-STEAM) MR spectroscopy to measure fat unsaturation in regions with low proton-density fat fraction, Magn. Reson. Med. 75 (1) (2015) 32–41.
[28] H. Eggers, P. Bornert, Chemical shift encoding-based water-fat separation methods, J. Magn. Reson. Imaging 40 (2) (2014) 251–268.
[29] B.L. Johnson, M.E. Schroeder, T. Wolfson, A.C. Gamst, G. Hamilton, M. Shiehmorteza, R. Loomba, J.B. Schwimmer, S. Reeder, M.S. Middleton, C.B. Sirlin, Effect of flip angle on the accuracy and repeatability of hepatic proton density fat fraction estimation by complex data-based, T1-independent, T2*-corrected, spectrum-modeled MRI, J. Magn. Reson. Imaging 39 (2) (2014) 440–447.
[30] D.C. Karampinos, S. Ruschke, M. Dieckmeyer, H. Eggers, H. Kooijman, E.J. Rummeny, J.S. Bauer, T. Baum, Modeling of T* decay in vertebral bone marrow fat quantification, NMR Biomed. 28 (11) (2015) 1535–1542.
[31] D.C. Karampinos, G. Melkus, T. Baum, J.S. Bauer, E.J. Rummeny, R. Krug, Bone marrow fat quantification in the presence of trabecular bone: initial comparison between water-fat imaging and single-voxel MRS, Magn. Reson. Med. 71 (3) (2014) 1158–1165.
[32] T. Baum, S.P. Yap, M. Dieckmeyer, S. Ruschke, H. Eggers, H. Kooijman, E.J. Rummeny, J.S. Bauer, D.C. Karampinos, Assessment of whole spine vertebral bone marrow fat using chemical shift-encoding based water-fat MRI, J. Magn. Reson. Imaging 42 (4) (2015) 1018–1023.
[33] L.M. Negrete, M.S. Middleton, L. Clark, T. Wolfson, A.C. Gamst, J. Lam, C. Changchien, I.M. Deyoung-Dominguez, G. Hamilton, R. Loomba, J. Schwimmer, C.B. Sirlin, Inter-examination precision of magnitude-based MRI for estimation of segmental hepatic proton density fat fraction in obese subjects, J. Magn. Reson. Imaging 39 (5) (2014) 1265–1271.
[34] H. Alizai, L. Nardo, D.C. Karampinos, G.B. Joseph, S.P. Yap, T. Baum, R. Krug, S. Majumdar, T.M. Link, Comparison of clinical semi-quantitative assessment of muscle fat infiltration with quantitative assessment using chemical shift-based water/fat separation in MR studies of the calf of post-menopausal women, Eur. Radiol. 22 (7) (2012) 1592–1600.
[35] D. Wald, B. Teucher, J. Dinkel, R. Kaaks, S. Delorme, H. Boeing, K. Seidensaal, H.P. Meinzer, T. Heimann, Automatic quantification of subcutaneous and visceral adipose tissue from whole-body magnetic resonance images suitable for large cohort studies, J. Magn. Reson. Imaging 36 (6) (2012) 1421–1434.
[36] B. Ludescher, J. Machann, G.W. Eschweiler, S. Vanhofen, C. Maenz, C. Thamer, C.D. Claussen, F. Schick, Correlation of fat distribution in whole body MRI with generally used anthropometric data, Invest. Radiol. 44 (11) (2009) 712–719.
[37] K. Kirchhoff, K. Kantartzis, J. Machann, F. Schick, C. Thamer, F. Machicao, A. Fritsche, H.U. Haring, N. Stefan, Impact of different fat depots on insulin sensitivity: predominant role of liver fat, J. Diabetes Sci. Technol. 1 (5) (2007) 753–759.
[38] J.A. Kanaley, I. Giannopoulou, L.L. Ploutz-Snyder, Regional differences in abdominal fat loss, Int. J. Obes. (Lond.) 31 (1) (2007) 147–152.
[39] C. Cordes, M. Dieckmeyer, B. Ott, J. Shen, S. Ruschke, M. Settles, C. Eichhorn, J.S. Bauer, H. Kooijman, E.J. Rummeny, T. Skurk, T. Baum, H. Hauner, D.C. Karampinos, MR-detected changes in liver fat, abdominal fat, and vertebral bone marrow fat after a four-week calorie restriction in obese women, J. Magn. Reson. Imaging 42 (5) (2015) 1272–1280.
[40] K. Fischer, J.A. Pick, D. Moewes, U. Nothlings, Qualitative aspects of diet affecting visceral and subcutaneous abdominal adipose tissue: a systematic review of observational and controlled intervention studies, Nutr. Rev. 73 (4) (2015) 191–215.
[41] D. Gallagher, S. Heshka, D.E. Kelley, J. Thornton, L. Boxt, F.X. Pi-Sunyer, J. Patricio, J. Mancino, J.M. Clark, Changes in adipose tissue depots and metabolic markers following a 1-year diet and exercise intervention in overweight and obese patients with type 2 diabetes, Diabetes Care 37 (12) (2014) 3325–3332.
[42] E. Bacchi, C. Negri, M.E. Zanolin, C. Milanese, N. Faccioli, M. Trombetta, G. Zoppini, A. Cevese, R.C. Bonadonna, F. Schena, E. Bonora, M. Lanza, P. Moghetti, Metabolic effects of aerobic training and resistance training in type 2 diabetic subjects: a randomized controlled trial (the RAED2 study), Diabetes Care 35 (4) (2012) 676–682.
[43] J.S. Bauer, P.B. Noel, C. Vollhardt, D. Much, S. Degirmenci, S. Brunner, E.J. Rummeny, H. Hauner, Accuracy and reproducibility of adipose tissue measurements in young infants by whole body magnetic resonance imaging, PLoS One 10 (2) (2015) e0117127.
[44] T.A. Harrington, E.L. Thomas, N. Modi, G. Frost, G.A. Coutts, J.D. Bell, Fast and reproducible method for the direct quantitation of adipose tissue in newborn infants, Lipids 37 (1) (2002) 95–100.
[45] T.A. Harrington, E.L. Thomas, G. Frost, N. Modi, J.D. Bell, Distribution of adipose tissue in the newborn, Pediatr. Res. 55 (3) (2004) 437–441.
[46] E. Olhager, E. Flinke, U. Hannerstad, E. Forsum, Studies on human body composition during the first 4 months of life using magnetic resonance imaging and isotope dilution, Pediatr. Res. 54 (6) (2003) 906–912.
[47] I.M. Schrover, T. Leiner, D.W. Klomp, J.P. Wijnen, C.S. Uiterwaal, W. Spiering, F.L. Visseren, Feasibility and reproducibility of free fatty acid profiling in abdominal adipose tissue with 1H-magnetic resonance spectroscopy at 3 T: differences between lean and obese individuals, J. Magn. Reson. Imaging 40 (2) (2014) 423–431.
[48] J. Machann, N. Stefan, C. Schabel, E. Schleicher, A. Fritsche, C. Wurslin, H.U. Haring, C.D. Claussen, F. Schick, Fraction of unsaturated fatty acids in visceral adipose tissue (VAT) is lower in subjects with high total VAT volume—a combined 1 H MRS and volumetric MRI study in male subjects, NMR Biomed. 26 (2) (2013) 232–236.
[49] Z. Dong, Y. Luo, Z. Zhang, H. Cai, Y. Li, T. Chan, L. Wu, Z.P. Li, S.T. Feng, MR quantification of total liver fat in patients with impaired glucose tolerance and healthy subjects, PLoS One 9 (10) (2014) e111283.
[50] K. Linder, F. Springer, J. Machann, F. Schick, A. Fritsche, H.U. Haring, G. Blumenstock, M.B. Ranke, N. Stefan, G. Binder, S. Ehehalt, Relationships of body composition and liver fat content with insulin resistance in obesity-matched adolescents and adults, Obesity (Silver Spring) 22 (5) (2014) 1325–1331.
[51] A. Kotronen, M. Peltonen, A. Hakkarainen, K. Sevastianova, R. Bergholm, L.M. Johansson, N. Lundbom, A. Rissanen, M. Ridderstrale, L. Groop, M. Orho-Melander, H. Yki-Jarvinen, Prediction of non-alcoholic fatty liver disease and liver fat using metabolic and genetic factors, Gastroenterology 137 (3) (2009) 865–872.
[52] J. Machann, C. Thamer, N. Stefan, N.F. Schwenzer, K. Kantartzis, H.U. Haring, C.D. Claussen, A. Fritsche, F. Schick, Follow-up whole-body assessment of adipose tissue compartments during a lifestyle intervention in a large cohort at increased risk for type 2 diabetes, Radiology 257 (2) (2010) 353–363.
[53] K. Kantartzis, J. Machann, F. Schick, K. Rittig, F. Machicao, A. Fritsche, H.U. Haring, N. Stefan, Effects of a lifestyle intervention in metabolically benign and malign obesity, Diabetologia 54 (4) (2011) 864–868.
[54] M. Boettcher, J. Machann, N. Stefan, C. Thamer, H.U. Haring, C.D. Claussen, A. Fritsche, F. Schick, Intermuscular adipose tissue (IMAT): association with other adipose tissue compartments and insulin sensitivity, J. Magn. Reson. Imaging 29 (6) (2009) 1340–1345.
[55] R. Sinha, S. Dufour, K.F. Petersen, V. LeBon, S. Enoksson, Y.Z. Ma, M. Savoye, D.L. Rothman, G.I. Shulman, S. Caprio, Assessment of skeletal muscle triglyceride content by (1)H nuclear magnetic resonance spectroscopy in lean and obese adolescents: relationships to insulin sensitivity, total body fat, and central adiposity, Diabetes 51 (4) (2002) 1022–1027.
[56] D.C. Karampinos, T. Baum, L. Nardo, H. Alizai, H. Yu, J. Carballido-Gamio, S.P. Yap, A. Shimakawa, T.M. Link, S. Majumdar, Characterization of the regional distribution of skeletal muscle adipose tissue in type 2 diabetes using chemical shift-based water/fat separation, J. Magn. Reson. Imaging 35 (4) (2012) 899–907.
[57] J.F. Griffith, D.K. Yeung, G.E. Antonio, S.Y. Wong, T.C. Kwok, J. Woo, P.C. Leung, Vertebral marrow fat content and diffusion and perfusion indexes in women with varying bone density: MR evaluation, Radiology 241 (3) (2006) 831–838.
[58] J.F. Griffith, D.K. Yeung, G.E. Antonio, F.K. Lee, A.W. Hong, S.Y. Wong, E.M. Lau, P.C. Leung, Vertebral bone mineral density, marrow perfusion, and fat content in healthy men and men with osteoporosis: dynamic contrast-enhanced MR imaging and MR spectroscopy, Radiology 236 (3) (2005) 945–951.
[59] M.A. Bredella, M. Torriani, R.H. Ghomi, B.J. Thomas, D.J. Brick, A.V. Gerweck, C.J. Rosen, A. Klibanski, K.K. Miller, Vertebral bone marrow fat is positively associated with visceral fat and inversely associated with IGF-1 in obese women, Obesity (Silver Spring) 19 (1) (2011) 49–53.
[60] M.A. Bredella, C.M. Gill, A.V. Gerweck, M.G. Landa, V. Kumar, S.M. Daley, M. Torriani, K.K. Miller, Ectopic and serum lipid levels are positively associated with bone marrow fat in obesity, Radiology 269 (2) (2013) 534–541.
[61] T. Baum, S.P. Yap, D.C. Karampinos, L. Nardo, D. Kuo, A.J. Burghardt, U.B. Masharani, A.V. Schwartz, X. Li, T.M. Link, Does vertebral bone marrow fat content correlate with abdominal adipose tissue, lumbar spine bone mineral density, and blood biomarkers in women with type 2 diabetes mellitus? J. Magn. Reson. Imaging 35 (1) (2012) 117–124.
[62] L. Sidossis, S. Kajimura, Brown and beige fat in humans: thermogenic adipocytes that control energy and glucose homeostasis, J. Clin. Invest. 125 (2) (2015) 478–486.
[63] M.J. Devlin, The Skinny on brown fat, obesity, and bone, Am. J. Phys. Anthropol. 156 (Suppl. 59) (2015) 98–115.
[64] D. Franz, D.C. Karampinos, E.J. Rummeny, M. Souvatzoglou, A.J. Beer, S.G. Nekolla, M. Schwaiger, M. Eiber, Discrimination between brown and white adipose tissue using a 2-Point dixon water-Fat separation method in simultaneous PET/MRI, J. Nucl. Med. 56 (11) (2015) 1742–1747.